International Journal of Earth, Energy and Environmental Sciences
ISSN: 2517-942X
Vol:9, No:12, 2015

Finite Element Modeling of the Mechanical Behavior of Municipal Solid Waste Incineration Bottom Ash with the Mohr-Coulomb Model

Le Ngoc Hung, Abriak Nor Edine, Binetruy Christophe, Benzerzour Mahfoud, Shahrour Isam, Patrice Rivard

***Abstract*—**Bottom ash from Municipal Solid Waste Incineration (MSWI) can be viewed as a typical granular material because these industrial by-products result from the incineration of various domestic wastes. MSWI bottom ash is mainly used in road engineering in substitution of the traditional natural aggregates. As the characterization of their mechanical behavior is essential in order to use them, specific studies have been led over the past few years. In the first part of this paper, the mechanical behavior of MSWI bottom ash is studied with triaxial tests. After, analysis of the experiment results, the simulation of triaxial tests is carried out by using the software package CESAR-LCPC. As the first approach in modeling of this new class material, the Mohr-Coulomb model was chosen to describe the evolution of material under the influence of external mechanical actions.

***Keywords*—**Bottom ash, granular material, triaxial test, mechanical behavior, simulation, Mohr-Coulomb model, CESAR-LCPC.

I. Introduction

MSWI bottom ash is the solid residue issue of the domestic waste combustion in the furnace of the incineration factory, which represents 25-30% in mass and 10 % in volume of incinerated wastes [1]-[3], [10], [11]. In France, about 3 million tons of bottom ash are annually produced [4], [5], [12], [13]. The increasing amount of the MSWI bottom ash production leads to two main issues, which are environmental impacts and limitation of the MSWI bottom ash storage. While the granulate quarry is becoming more and more nearly exhausted, it is difficult to create new quarries in the context of sustainable development.

Currently MSWI bottom ash is mainly used in the domain of civil engineering for realizing embankments, road layers and parkings areas, etc. [6], [14], [26]-[31]. But the mechanical properties of MSWI bottom ash are still poorly known (empirical use) even if some studies of MSWI bottom ash have provided very encouraging results mainly on the experimental aspects [2], [7], [20]-[25]. However, the selection and the development of an appropriate model suitable for the specific "MSWI bottom ash" have never been proposed to our best knowledge.

The first part is to achieve the characterization of the mechanical behaviors of MSWI bottom ash under triaxial tests. Then the triaxial tests are simulated by using the finite element software package CESAR-LCPC. The Mohr-Coulomb model is chosen to characterize the evolution of material under the influence of external mechanical loadings. This model, suitable for perfect elastoplastic materials, is commonly used in civil engineering to assess the behavior of granular soils (sand and gravel) and the long-term drained behavior of saturated soils (silt and clay) [34]. Moreover, using the law of Mohr-Coulomb behavior of not knowing very well the characteristics of bottom ash, the error committed in considering this law is not the same as the one introduced by the ignorance of bottom ash and the baseline condition for such calculation. Furthermore, starting of modeling with the basic and classic Mohr-Coulomb model helps to work more easily with the behavior model more complexity like the Nova behavior model and the Vermeer behavior model.

II. Studied Material

This studied MSWI bottom ash is supplied by PréferNord (France) and sorted to remove ferrous elements, aluminium and heavy elements (Fig. 1). According to the classification of *technical guide SETRA-LCPC* [14], it is a bottom ash of type V, which can be used in civil engineering such as trench backfills or sub-layers of pavement, in place of finer materials such as sand or gravel.

Fig. 1 MSWI bottom ash after treatments

III. Triaxial Tests

The data of triaxial tests set is reported in Table I. The set A

Abriak Nor-Edine and Benzerzour Mahfoud are with the Mines de Douai, France (Corresponding author: Abriak Nor-Edine, e-mail: nor-edine.abriak@mines-douai.fr, mahfoud.benzerzour@mines-douai.fr).
Le Ngoc Hung was with the Mines de Douai, France (e-mail: lipton_estc@yahoo.fr).
Binetruy Christophe is with the Ecole Centrale de Nantes, France (e-mail: christophe.binetruy@ec-nantes.fr).
Shahrour Isam is with the Université de Lille 1, France (e-mail: isam.shahrour@univ-lille1.fr).
Patrice Rivard is with the Université de Sherbrooke, Canada (Patrice.Rivard@USherbrooke.ca).

of consolidated-drained triaxial tests is performed with the pore pressures equal to u = 200 kPa. The effective confining pressure varies from p' = 100 kPa to p' = 400 kPa in steps of 100 kPa. In fact, many sets of consolidated-drained triaxial tests were tested, only one of them with the pore pressures equal to u = 200 kPa is reported and discussed hereafter. The deviatoric stress and the volumetric strain versus axial strain curves obtained from the triaxial test sets are represented in Figs. 2 (a), (b).

TABLE I
TESTING CONDITIONS FOR THE TRIAXIAL TESTS SET A

Test	u (kPa)	σ_3 (kPa)	p' (kPa)
A1	200	300	100
A2	200	400	200
A3	200	500	300
A4	200	600	400

The typical stress-strain responses reported in Figs. 2 (a) and (b) indicate that the mechanical behavior is similar to that of dense sands [15]-[17], [20], [25]. The comparison of the deviatoric stress evolution for the tests A indicates that the curves are really similar in terms of trend and quantitative results (Fig. 2 (a)). The first phase is almost linear up to 70% of the peak deviatoric stress and second non-linear phase is progressive to the peak deviatoric stress. Finally, there is a final phase where the curves tend towards a level characterized by a residual deviatoric stress. In Fig. 2 (b), the strain curves show an initial phase of contracting followed by a phase of dilatancy for large strains. If tests are conducted on large strains without localization phenomenon, it can be assumed that all the curves tend towards a horizontal asymptote (critical). Triaxial test results are used to select a mechanical model adapted to the granular material "MSWI bottom ash". The Mohr-Coulomb model is chosen as a first approach for the MSWI bottom ash.

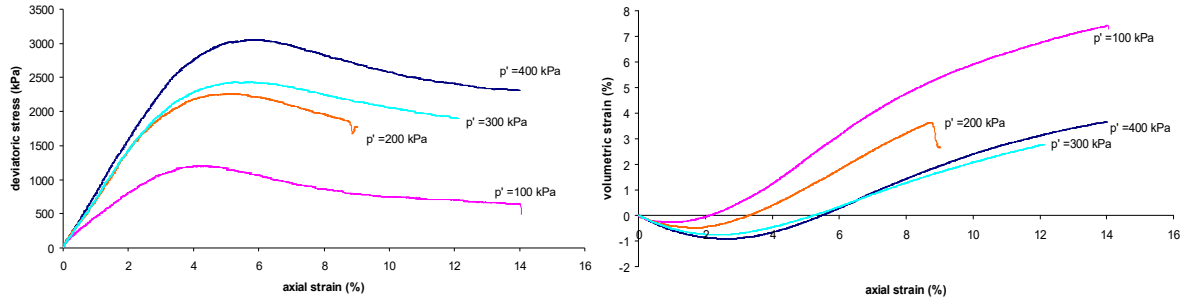

(a) (b)

Fig. 2 (a) Evolution of the deviatoric stress in the triaxial test set A (b) Evolution of the volumetric strain in the triaxial test set A

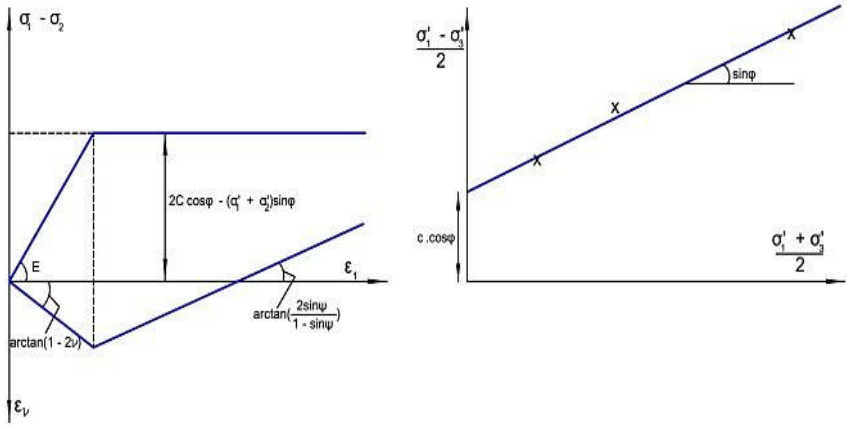

Fig. 3 Representation of the elastoplastic Mohr-Coulomb behavior law with its parameters

TABLE II
VALUES OF PARAMETERS IN THE MOHR-COULOMB MODEL

Test	E (MPa)	ν	ψ (°)	φ (°)	c (MPa)
A1	42.56	0.198	11.36	54.53	0
A2	70.01	0.235	13.28	54.53	0
A3	73.22	0.206	11.01	54.53	0
A4	79.98	0.197	12.46	54.53	0

IV. DETERMINATION OF MECHANICAL PARAMETERS

The elastoplastic Mohr-Coulomb model has five parameters, which are the Young modulus E, the Poisson coefficientν, the characteristic angleφ, the dilatancy angle ψ and the cohesion c [32], [33]. Fig. 3 graphically presents the significance of the Mohr-Coulomb behavior law and the

definition of Mohr-Coulomb law parameters.

Table II reports the values of parameters in the Mohr-Coulomb model for the triaxial test set A.

V. Modeling

A. Digital Tools

CESAR-LCPC is a generic finite element software package for solving different types of problems in mechanics, diffusion of fluids and heat and coupled problems. Its main application areas are related to civil and environment engineering to perform calculation by construction phases and achieve analysis in hydrogeology, heat transfer, soil mechanics and rocks, structural analysis, etc. [8], [18], [19].

B. Simulation of Drained Triaxial Tests

The geometrical model consists of a cylindrical domain (117.5 mm in height and 111.5 mm in diameter), where only one quarter is modeled due to the symmetry (Fig. 4).

The mesh is made of an 8-nodes quadratic element referenced MBQ8. The stress fields applied during the triaxial test on the studied sample are considered sufficiently homogeneous to be viewed as unique stress and deformation tensors, independent of the considered point [32]. This fact explains why we only modeled the specimen by one element.

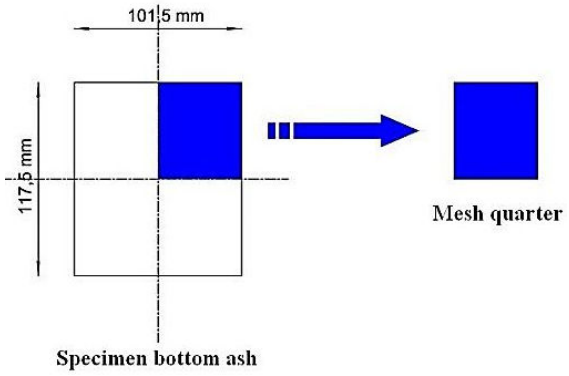

Fig. 4 Geometric model of the modeling

In all simulations, the horizontal displacement of the left edge of the mesh (that coincides with the axis of the rotational symmetry) is zero; a zero vertical displacement at the base of the mesh is also imposed (Fig. 5). Then, two uniform pressures, which correspond to the effective confinement pressure, are applied at the top edge and the right edges.

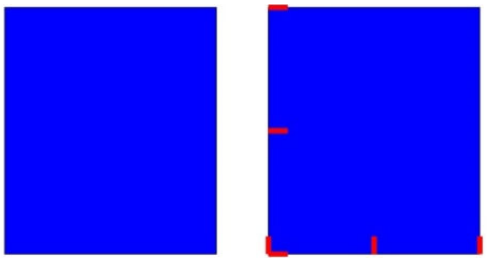

Fig. 5 Model mesh and boundary conditions

The loading cycle is carried out in two successive steps: one confining mode by applying an isotropic stress followed by a shear phase by applying of constant axial displacement rate. To obtain the plasticity level of the Mohr-Coulomb law, the simulation of the shear phase is performed by imposed displacement [9] (Fig. 6).

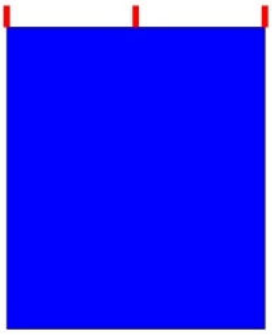

Fig. 6 Procedure of the model loading

C. Presentation of Calculation Results and Discussion

Figs. 7-10 present the simulation results of the drained triaxial tests set. The comparison between the experimental results and the simulations shows that the Mohr-Coulomb model qualitatively matches the experimental data. However some differences are quantitatively noted in terms of the initial elastic modulus, the shear strength and the contraction/dilatancy.

For the evolution of deviator stress curves with the Mohr-Coulomb model, it has not been used to simulate the observed experimental concavity. For tests with a small effective confining pressure p' = 100 kPa and 200 kPa (test A1, A2), the simulations underestimate the deviatoric stress value at the failure point (Figs. 7 (a), 8 (a)). For tests with a medium effective confining pressure p' = 300 kPa and 400 kPa (test A3, A4), the simulations overestimate the deviatoric stress value at the failure point (Figs. 9 (a), 10 (a)).

The Mohr-Coulomb model overestimates the measured shear dilatancy (Figs. 7 (b), 10 (b)).

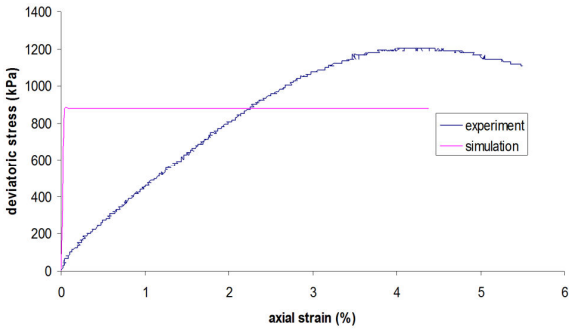

(a)

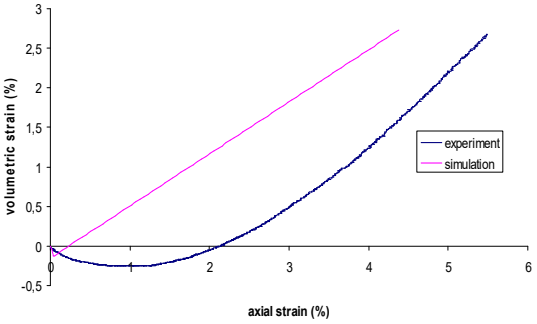

(b)

Fig. 7 (a) Evolution of the deviatoric stress in the test A1 (simulation and experiment) (b) Evolution of the volumetric strain in the test A1 (simulation and experiment)

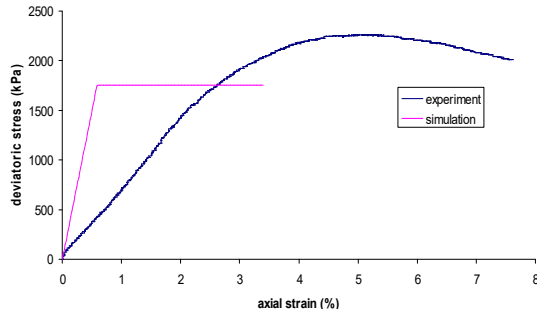

(a)

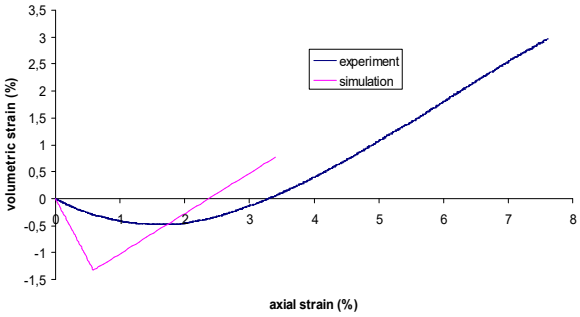

(b)

Fig. 8 (a) Evolution of the deviatoric stress in the test A2 (simulation and experiment) (b) Evolution of the volumetric strain in the test A2 (simulation and experiment)

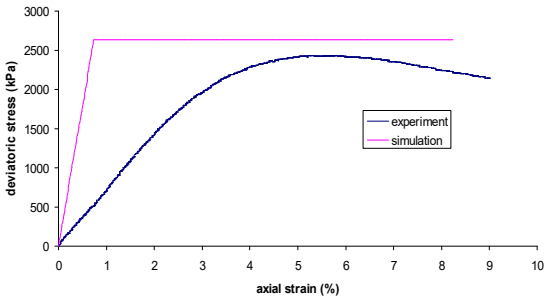

(a)

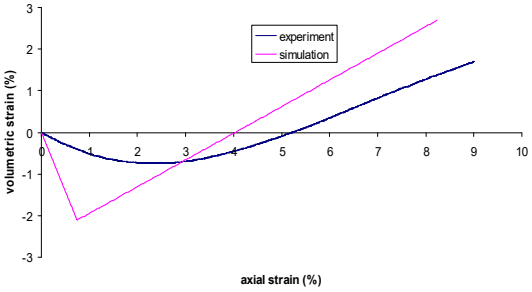

(b)

Fig. 9 (a) Evolution of the deviatoric stress in the test A3 (simulation and experiment) (b) Evolution of the volumetric strain in the test A3 (simulation and experiment)

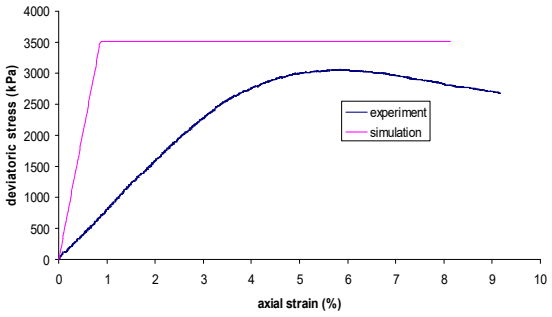

(a)

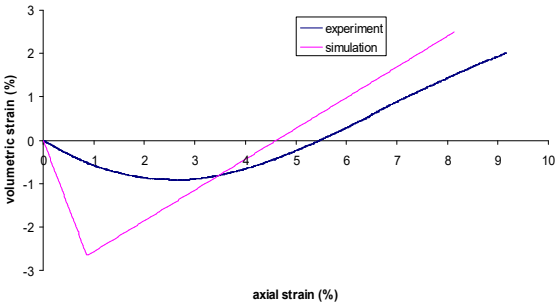

(b)

Fig. 10 (a) Evolution of the deviatoric stress in the test A4 (simulation and experiment) (b) Evolution of the volumetric strain in the test A4 (simulation and experiment)

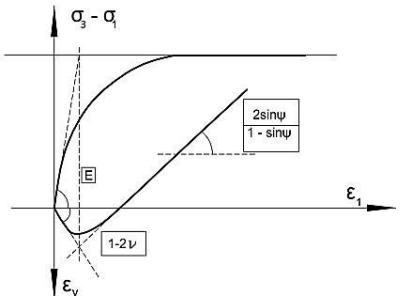

Fig. 11 Analysis of the material state according to the evolution of the volumetric strain

D.Parametric Optimisation of the Mohr-Coulomb Law

According to the basic principle of the Mohr-Coulomb model, the material in the soil massif is at either the elastic or plastic state. This distinction can be obviously made by analyzing the evolution of the axial strain and of the volumetric strain. Two options that show two different graphical interpretations are given in Figs. 11 and 12.

- Option 1: Elastic - plastic transition monitored by the evolution of volumetric strain.
- Option 2: Elastic - plastic transition monitored by the evolution of the axial stress: The Poisson coefficient is adapted to respect the maximum value of volumetric strain f the environmental impacts as the mechanical behavior, it seems important at this stage to investigate the behavior of designed material in the framework of a monitored experimental road.

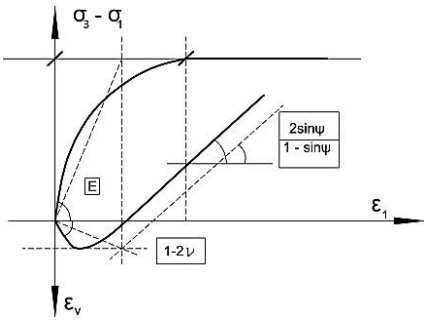

Fig. 12 Analysis of the material state according to the evolution of the deviatoric stress and the maximum value of volumetric strain

The test A2 is chosen to run the optimisation procedure. Table III presents the parameters obtained using the two options.

Figs. 13 (a) and (b) show the results of the parametric optimisation of the Mohr-Coulomb model in terms of the evolution of the deviatoric stress. The difference between the results obtained from the "original" parameters and the "option 1" and "option 2" parameters is not important. Predictions obtained with the "option 1" parameters are closer to the experimental results at the maximum volumetric strain.

A. Sensitivity Analysis

The Mohr-Coulomb model cannot give consistent results because it ignores some important aspects such as the heterogeneity of a by-product. On the other hand, like any model, its accuracy depends on the values of the input parameters. A systematic parametric study is then undertaken on the basis of simulations of drained triaxial test.

TABLE III
DATA SET CORRESPONDING TO TWO OPTIONS

Test	Option	E (MPa)	ν
A2	Original	70.01	0.235
	Option 1	131.29	0.235
	Option 2	70.01	0.094

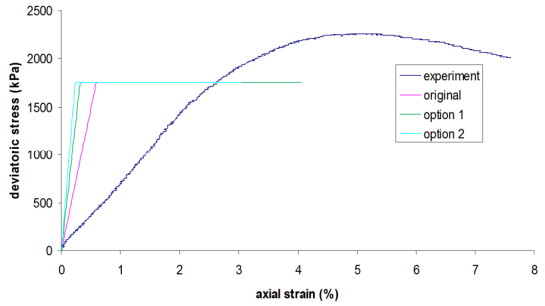

(a)

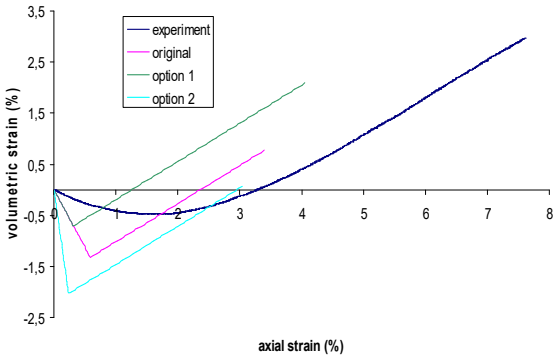

(b)

Fig. 13 (a) Simulation of the test A2 according "original", "option 1" and "option 2" parameters (evolution of the deviatoric stress) (b) Simulation of the test A2 according "original", "option 1" and "option 2" parameters (evolution of the volumetric strain)

1) Selection of parameters

In this sensitivity, each parameter is varied from % while keeping other parameters at constant. Values of selected parameters are displayed in Table IV.

TABLE IV
SELECTED PARAMETERS VALUES OF THE MOHR-COULOMB LAW FOR THE PARAMETRIC STUDY

Parameters	*E* (MPa)	ν	ψ (°)	φ (°)	*c* (MPa)
Reference values	65	0.20	12.5	55	0
-25 %	50	0.15	9.5	50	0
+25 %	80	0.25	15.5	60	0

2) Synthesis of Results

The main conclusions drawn from the sensitivity analysis and the detailed results are summarized in Tables V and VI and in Figs. 14-17.

TABLE V
EFFECT OF CHANGES OF PARAMETERS VALUES ON THE DEVIATORIC STRESS CURVE

	Type of the influence
E	The increase in E causes an increase of the initial slope of the curve but no difference between the deviator values at the large deformation
ν	The increase in ν causes an increase of the initial slope of the curve but no difference between the deviator values at the large deformation
ψ	No influence on the entire curve
φ	Major influence on the deviator level at the failure point

TABLE VI
EFFECT OF CHANGES OF PARAMETERS VALUES ON THE STRAIN CURVE

	Type of the influence
E	Significant influence on the characteristic state of the curve
ν	The increase in E causes an increase of the initial slope of the curve and an average influence on the characteristic state
ψ	Large influence on the slope of the curve after the characteristic state
φ	Significant influence on the characteristic state of the curve

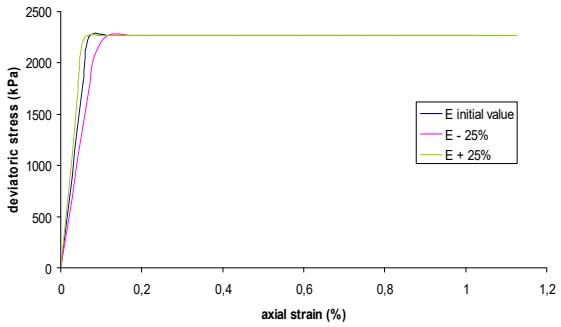

(a)

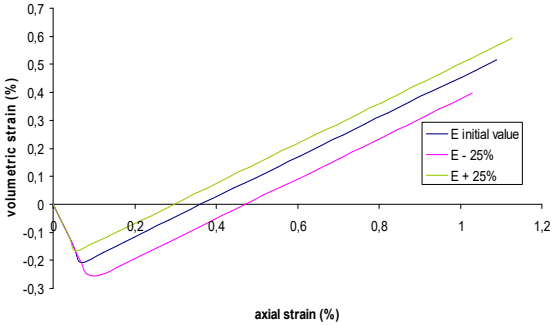

(b)

Fig. 14 (a) Influence of E on the deviatoric stress curve (b) Influence of E on the strain curve

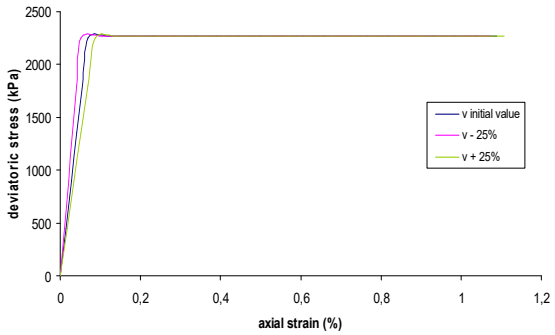

(a)

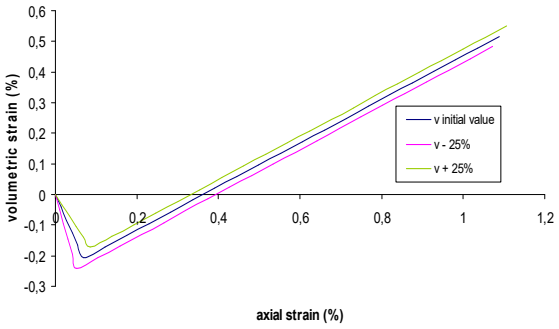

(b)

Fig. 15 (a) Influence of ν on the deviatoric stress curve (b) Influence of ν on the strain curve

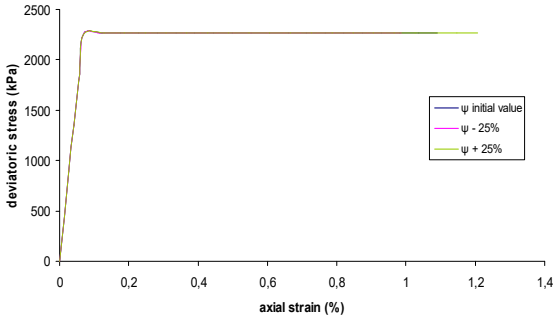

(a)

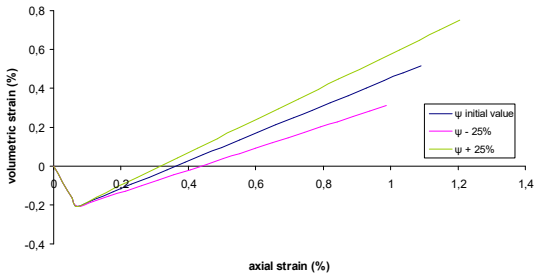

(b)

Fig. 16 (a) Influence of ψ on the deviatoric stress curve (b) Influence of ψ on the strain curve

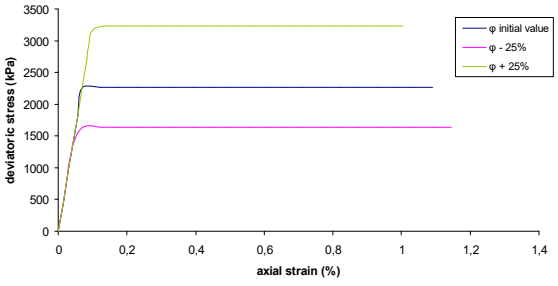

(a)

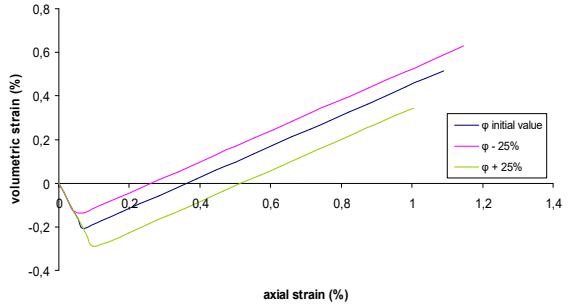

(b)

Fig. 17 (a) Influence of φ on the deviatoric stress curve (b) Influence of φ on the strain curve

VI. Conclusions

Triaxial tests on MSWI bottom ash were experimentally run and then modeled with the Mohr-Coulomb law. The simulations were performed using the CESAR-LCPC software package.

The comparison between the experimental results and simulations shows that the Mohr-Coulomb model is able to qualitatively capture the obtained experimental trends. However, some quantitative differences are reported in terms of the initial elasticity modulus, the shear strength and the contraction/dilatancy. The Mohr-Coulomb law cannot capture the concavity observed in the deviatoric stress curves. Predictions underestimate or overestimate the deviatoric stresses at the failure point depending on the effective confining pressure applied. There is a poor agreement between the experimental and simulated evolution of strain curves. Finally, it has been shown that the Mohr-Coulomb model overestimates the shear dilatancy.

A sensibility analysis of the model parameter has been conducted to detect the dominant factors and to improve the model predictions. It is concluded that variations of each parameter modify at least one mechanical output (shear and volume).

All these findings give the evidence that an elastoplastic model with hardening would be more appropriate. The Nova's model has been developed to describe the mechanical behavior of dense sands from triaxial tests (reference for the Nova's model). Given its mechanical behavior, MSWI bottom ash would be better modeled with the Nova's law. This will be a topic for a future study.

References

[1] J. M. Chimenos, A. I. Fernandez, R. Nadal, F. Espiell. Short-term natural weathering of MSWI bottom ash. *Journal of Hazardous Materials B* 2000; 79: 287-299.
[2] M. Arm. Variation in deformation properties of processed MSWI bottom ash: results from triaxial tests. *Waste Management* 2004; 24: 1035-1042.
[3] K. O. Joar, G. Elin, M. Amund. Mass-balance estimation of heavy metals and selected anions at a landfill receiving MSWI bottom ash and mixed construction wastes. *Journal of Hazardous Materials A* 2005; 123: 70-75.
[4] Ademe Itom. *Les installations de traitement des ordures ménagères 2008*.
[5] N. Lapa, R. Barbosa, J. Morais, B. Mendes, J. Méhu, J. F. S. Oliveira. Ecotoxicological assessment of leachates from MSWI bottom ashes. *Waste Management* 2002; 22: 583-593.
[6] Ademe Brgm. *Mâchefers d'incinération des ordures ménagères. Etat de l'art et perspectives* 2008.
[7] F. Becquart, F. Bernard, N. E. Abriak, R. Zentar. Monotonic aspects of the mechnical behaviour of bottom ash grom municipal solid waste incineration and its potential use for road construction. *Waste Management* 2008; 29: 1320-1329.
[8] CESAR-LCPC. CESAR-LCPC, un progiciel de calcul dédié au génie civil. *Bulletin des LPC* -256-267 Juillet-Août-Septembre 2005 –RRF; 4573: 7-37.
[9] P. Mestat, P. Humbert. Référentiel de tests pour la vérification de la programmation des lois de comportement dans les logiciels d'éléments finis. *Bulletins des LPC* -230 2001.
[10] J. M. Chimenos, M. Segarra, M. Fernandez, F. Espiell. Characterization of the bottom ash in municipal solid waste incinerator. *Journal of Hazardous Materials A* 1999; 64: 211-222.
[11] R. Ibanez, A. Andrés, J. R. Viguiri, I. Ortiz, J. A. Irabien. Characterization and management of incinerator wastes. *Journal of Hazardous Materials A* 2000; 79: 215-227.
[12] Ademe Itom. *Les installations de traitement des ordures ménagères* 2004.
[13] Ademe Itom. *Les installations de traitement des ordures ménagères* 2006.
[14] SETRA-LCPC. *Guide technique SETRA D9233-1*. Réalisation des remblais et des couches de forme. Fascicule I.
[15] M. P. Luong. Phénomène cyclique dans les sols pulvérulents. Revue *Française de Géotechnique* 1980; 10: 39-53.
[16] M. Prat. *La modélisation des ouvrages AFPC*. Emploi des éléments finis en génie civil 1995.
[17] P. Evesque. *Eléments de mécanique quasi-statique des milieux granulaires mouillés ou secs*. Mécanique des milieux granulaires 2000; 157 pages.
[18] CESAR-LCPC, 2002a. *CESAR-LCPC version 4.0, Manuel de référence du solveur*. Lcpc – Itech 2002.
[19] CESAR-LCPC, 2002b. *CESAR-LCPC version 4.0, Manuel de référence CLEO2D*. Lcpc – Itech 2002.
[20] F. Becquart. Comportement mécanique au triaxial d'un mâchefer d'incinération d'ordures ménagères. *European journal of environmental and civil engineering* 2008; 2: issue 6.
[21] N. H. Le, N. E. Abriak, C. Binetruy, M. Benzerzour, S. Chaki. The study of behavior of bottom ash under homogeneous stresses. Determination of parameters for Nova behavior models. *Proceeding of Euromediterranean Symposium on Advances in Geomaterials and Structures*, Djerba, Tunisia 2010, 653-660.
[22] N. H. Le, N. E. Abriak, M. Benzerzour, C. Binetruy, M. L. Nguyen. Influence of loading rate on mechanical behaviour of a bottom ashes from municipal solid waste incineration in a triaxial test. *Proceeding of the Geotechnics for Suitainable Development – Geotec Hanoi* 2011, Vietnam 2011, 651-658.
[23] F. Bernard., N. E. Abriak. Étude physique, géotechnique, et mécanique d'un mâchefer d'incinération d'ordures ménagères. *Journal of catalytic materials and environment* 2003; 1: 9-18.
[24] C. Caroline. *Étude expérimentale du gonflement des Mâchefers d'Incinération d'Ordures Ménagères traités aux liants hydrauliques*. Thèse de doctorat, Université des Sciences et Techniques de Lille 2000; 144 pages.
[25] N. H. Le, N. E. Abriak, M. Benzerzour, C. Binetruy. Comportement mécanique d'un mâchefer d'incinération d'ordure ménagers. *Journal of catalytic materials and environment* 2012; 10: 3-12.
[26] H. Birgisdottir, G. Bhander, M. Z. Hauschild, T. H. Christensen. Life cycle assessment of disposal of residues from municipal solid waste incineration: Recycling of bottom ash in road construction or landfilling in Denmark evaluates in the ROAD-RES model. *Waste Management* 27 (2007) 75-84.
[27] R. Forteza, M. Far, C. Segui, V. Cerda. Characterization of bottom ash in municipal solid waste incinerators for its use un road base. *Waste Management* 24 (2004) 899-909.
[28] O. Hjelmar. Waste Management in Denmark. *Waste Management* 1996; 6: 389-394.
[29] J. A. Meima, R. N. J. Comans. Overview of geochemical processes controlling leaching characteristics of MSWI bottom ash. *Waste Materials in Construction : Putting Theory into Practice* 1997.

[30] Note SETRA. *Note d'information: Utilisation des mâchefers d'incinération d'ordures ménagères en technique routière. SETRA-CSTR, Août* 1997.
[31] GTIF. *Guide technique pour l'utilisation des matériaux régionaux d'Ile-de-France.* Catalogue des structures de chaussées. Décembre 2003.
[32] P. Mestat. Lois de comportement des géomatériaux et modélisation par la méthode des éléments finis. ERLPC Série géotechnique, ISSN 1157-3910, mars 1993, 193 pages.
[33] P. Mestat. Méthodologie de détermination des paramètres des lois de comportement à partir d'essais triaxiaux conventionnels, *Rapport interne LPC*, 1990, FAER, 1.16.21.0.
[34] P. Mestat. *Étude du comportement des sables sous sollicitations homogènes*. Mémoire de DEA d'Emile Youssef (École Centrale de Paris) 1992, 169 pages.